



Published as: *J Am Chem Soc.* 2008 September 3; 130(35): 11576–11577.

## Direct In-Gel Fluorescence Detection and Cellular Imaging of *O*-GlcNAc-Modified Proteins

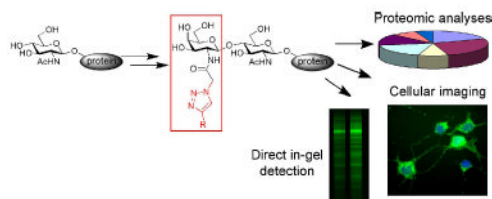
Peter M. Clark<sup>†</sup>, Jessica F. Dweck<sup>†</sup>, Daniel E. Mason<sup>‡</sup>, Courtenay R. Hart<sup>§</sup>, Suzanne B. Buck<sup>§</sup>, Eric C. Peters<sup>‡</sup>, Brian J. Agnew<sup>§</sup>, and Linda C. Hsieh-Wilson<sup>†,\*</sup>

<sup>†</sup>*Division of Chemistry and Chemical Engineering and Howard Hughes Medical Institute, California Institute of Technology, Pasadena, California 91125*

<sup>‡</sup>*Genomics Institute of the Novartis Research Foundation, San Diego, California 92121*

<sup>§</sup>*Invitrogen Corporation, Eugene, Oregon 97402*

### Abstract



We report an advanced chemoenzymatic strategy for the direct fluorescence detection, proteomic analysis, and cellular imaging of *O*-GlcNAc-modified proteins. *O*-GlcNAc residues are selectively labeled with fluorescent or biotin tags using an engineered galactosyltransferase enzyme and [3+2] azide-alkyne cycloaddition chemistry. We demonstrate that this approach can be used for direct in-gel detection and mass spectrometric identification of *O*-GlcNAc proteins, identifying 146 novel glycoproteins from the mammalian brain. Furthermore, we show that the method can be exploited to quantify dynamic changes in cellular *O*-GlcNAc levels and to image *O*-GlcNAc-glycosylated proteins within cells. As such, this strategy enables studies of *O*-GlcNAc glycosylation that were previously inaccessible and provides a new tool for uncovering the physiological functions of *O*-GlcNAc.

Understanding posttranslational modifications to proteins is critical for elucidating the functional roles of proteins within the dynamic environment of cells. *O*-Linked  $\beta$ -*N*-acetylglucosamine (*O*-GlcNAc) glycosylation has emerged as important for the regulation of diverse cellular processes, including transcription, cell division, and glucose homeostasis.<sup>1</sup> While new chemical tools have provided rapid, sensitive methods for detecting the modification and enabled better control over the activity of *O*-GlcNAc enzymes,<sup>1a,2</sup> significant challenges remain with regard to elucidating the functions of *O*-GlcNAc in cells. For instance, a robust method for the direct fluorescence detection of *O*-GlcNAc proteins in gels would permit monitoring of changes in glycosylation levels in response to cellular stimuli and greatly extend the reach of existing technologies. Furthermore, new tools for imaging *O*-GlcNAc-glycosylated proteins would enable the expression and dynamics of the modification to be monitored in cells and tissues. Here, we report an advanced chemoenzymatic labeling strategy that addresses these important needs.

Previous studies have shown that an engineered  $\beta$ -1,4-galactosyltransferase enzyme (Y289L GalT) efficiently transfers a ketogalactose moiety from an unnatural UDP substrate selectively onto *O*-GlcNAc-modified proteins.<sup>2a</sup> However, treatment of cell lysates with an aminoxy fluorescein derivative resulted in some nonspecific labeling of proteins. We therefore investigated whether Y289L GalT would accept the UDP-azidogalactose substrate **1** (UDP-GalNAz), which would allow for labeling of *O*-GlcNAc proteins using [3+2] azide-alkyne cycloaddition chemistry (Figure 1A).<sup>3</sup> In addition to providing alternative dyes to potentially reduce nonspecific interactions, this Cu(I)-catalyzed cycloaddition reaction would have the advantage of being performed more rapidly and at physiological pH.

We tested the approach using  $\alpha$ -crystallin, a known *O*-GlcNAc-modified protein with a low extent (~10%) of glycosylation.  $\alpha$ -Crystallin was treated with **1** and Y289L GalT, followed by reaction with CuSO<sub>4</sub>, sodium ascorbate, and the biotin-alkyne derivative **2** for 1 h at 25 °C. Analysis by gel electrophoresis and blotting with streptavidin conjugated to an IR680 dye showed robust, selective labeling of  $\alpha$ -crystallin, with no nonspecific labeling in the absence of GalT, **1** or **2** (Figure 1B). Notably, as little as 250 fmol of  $\alpha$ -crystallin (~25 fmol of glycosylated protein) was detectable, highlighting the sensitivity of the approach. In contrast, other methods such as *O*-GlcNAc antibodies or lectins failed to detect even 10  $\mu$ g (500 pmol) of  $\alpha$ -crystallin (Figure S1).<sup>2a</sup>

We next examined whether this approach could be used for direct in-gel fluorescence detection and proteome-wide analyses of *O*-GlcNAc-glycosylated proteins. Nuclear and cytosolic protein fractions from rat forebrain were azide-labeled and then reacted with the tetramethyl-6-carboxyrhodamine (TAMRA)-alkyne derivative **3**. The *O*-GlcNAc proteins were enriched by immunoprecipitation using an anti-TAMRA antibody to remove non-glycosylated proteins, resolved by 1D or 2D gel electrophoresis, and visualized by in-gel fluorescence imaging (Figures 2A, S2 and S3). Importantly, minimal nonspecific labeling was detected with the TAMRA-alkyne dye (Figure 2A, -GalT control lanes), and we observed efficient capture and enrichment of the TAMRA-labeled proteins (+GalT, eluent and flow-through lanes).

To identify *O*-GlcNAc proteins, bands from the gel were excised, proteolytically digested, and subjected to nanoLC-MS/MS analysis. The data acquisition and subsequent database searching methodologies employed are detailed in the Supporting Information. In total, we identified 213 proteins, representing 67 previously known and 146 novel, putative *O*-GlcNAc-modified proteins (Table S1). The majority of the proteins identified participate in neuronal signaling and synaptic function, suggesting important functional roles for *O*-GlcNAc in neuronal communication (Figure 2B). Surprisingly, in contrast to previous proteomic analyses of brain tissue,<sup>2b,4</sup> we identified many proteins involved in metabolism and biosynthesis, consistent with roles for *O*-GlcNAc in nutrient sensing and cell survival observed in other tissues.<sup>1</sup> Interestingly, the metabolic proteins included 9 of the 10 enzymes required for glycolysis, suggesting a previously unidentified level of control by *O*-GlcNAc of this pathway. Thus, the approach enables the identification of a large number of unique *O*-GlcNAc-modified proteins and has the advantages of ease and accessibility (e.g., short incubation times, simple gel-based detection and separation versus multiple chromatography steps, high-throughput analyses, commercially available reagents).

Understanding the cellular dynamics of *O*-GlcNAc glycosylation will be critical for elucidating its functional roles in both physiological and diseased states. However, few methods exist for quantifying changes in *O*-GlcNAc glycosylation in response to cellular stimuli. Glycosylation levels are typically monitored by immunoblotting with a general *O*-GlcNAc antibody,<sup>5</sup> which detects only a limited number of *O*-GlcNAc proteins and affords no opportunity to identify proteins undergoing changes in glycosylation. We examined whether our chemoenzymatic approach could overcome such limitations.

HeLa cells were stimulated with PUGNAc (*O*-(2-acetamido-2-deoxy- $\beta$ -D-glucopyranosylidene) amino-*N*-phenylcarbamate), an inhibitor of the  $\beta$ -*N*-acetylglucosaminidase enzyme that removes *O*-GlcNAc, and the *O*-GlcNAc-modified proteins were labeled and analyzed as before. PUGNAc treatment resulted in a  $163 \pm 3\%$  increase in overall *O*-GlcNAc glycosylation levels as measured by in-gel fluorescence analysis, and interestingly, ranged from 136-176%, depending on the specific protein (Figure 3A). The varying extent to which *O*-GlcNAc is induced upon cellular stimulation may indicate complex regulatory control of the modification. Thus, this approach provides a new method to visualize and quantify dynamic changes in protein *O*-GlcNAc glycosylation which, when coupled with in-gel digestion and MS analyses as described above, will enable the identification of specific proteins undergoing those changes.

Finally, we examined whether *O*-GlcNAc-modified proteins could be chemoenzymatically tagged and imaged in cells. HeLa cells and cultured cortical neurons were fixed, permeabilized, and labeled with **1** and Y289L GalT, followed by biotin-alkyne **2** or TAMRA-alkyne **3**. The biotin-treated cells were further incubated with a streptavidin-AlexaFluor 488 conjugate. Notably, addition of exogenous GalT and **1** to the cells led to robust labeling of *O*-GlcNAc-glycosylated proteins (Figure 3B). Although the TAMRA-alkyne **3** produced background labeling in the absence of **1** (data not shown), strong staining and minimal background labeling were observed using biotin-alkyne **2**. Consistent with the reported localization of *O*-GlcNAc enzymes,<sup>1a,c</sup> *O*-GlcNAc-glycosylated proteins were found in both the nucleus and cytoplasm. Moreover, we observed robust staining of proteins along neuronal processes, corroborating our mass spectrometric identification of many *O*-GlcNAc proteins involved in synaptic signaling. This is the first example of exploiting chemical tagging methods to image *O*-GlcNAc-modified proteins within cells.

In summary, we describe an advanced chemoenzymatic approach that exploits [3+2] cycloaddition chemistry to attach fluorescent and biotin tags to *O*-GlcNAc residues. Unlike other strategies such as metabolic labeling using GlcNAz sugars,<sup>6</sup> this method affords near quantitative labeling, does not perturb signaling pathways, and is amenable to all cell types and tissues. We show that the approach enables studies of *O*-GlcNAc glycosylation that were previously inaccessible. The ability to tag proteins selectively with a fluorescent reporter group permits rapid in-gel detection of *O*-GlcNAc proteins, facilitating proteomic analyses and providing a new method to quantify dynamic changes in glycosylation. Covalent labeling of proteins allows for cellular imaging of *O*-GlcNAc proteins in their native biological environment. Finally, this approach was developed in conjunction with researchers at Invitrogen with the goal of providing commercially available reagents that are now accessible to the wider research community. We anticipate that this new approach will be a powerful tool for advancing our understanding of the physiological functions and dynamic regulation of *O*-GlcNAc glycosylation within cells.

## Supplementary Material

Refer to Web version on PubMed Central for supplementary material.

## Acknowledgements

We thank Dr. P. Qasba for providing the mutant GalT plasmid, J. Rexach for providing neurons and helpful discussions, T. Nyberg for helpful discussions, and Prof. N. Pierce for use of the FujiFilm imager. This work was supported by the NIH (RO1 GM084724) and Howard Hughes Medical Institute.

## References

1. (a) Rexach JE, Clark PM, Hsieh-Wilson LC. *Nat Chem Biol* 2008;4:97–106. [PubMed: 18202679] (b) Hart GW, Housley MP, Slawson C. *Nature* 2007;446:1017–22. [PubMed: 17460662] (c) Love DC, Hanover JA. *Sci STKE* 2005;312:re13. [PubMed: 16317114]
2. (a) Khidekel N, Arndt S, Lamarre-Vincent N, Lippert A, Poulin-Kerstien KG, Ramakrishnan B, Qasba PK, Hsieh-Wilson LC. *J Am Chem Soc* 2003;125:16162–3. [PubMed: 14692737] (b) Khidekel N, Ficarro SB, Peters EC, Hsieh-Wilson LC. *Proc Natl Acad Sci USA* 2004;101:13132–7. [PubMed: 15340146] (c) Vocadlo DJ, Hang HC, Kim EJ, Hanover JA, Bertozzi CR. *Proc Natl Acad Sci USA* 2003;100:9116–21. [PubMed: 12874386] (d) Gross BJ, Kraybill BC, Walker S. *J Am Chem Soc* 2005;127:14588–9. [PubMed: 16231908] (e) Macauley MS, Whitworth GE, Debowski AW, Chin D, Vocadlo DJ. *J Biol Chem* 2005;280:25313–22. [PubMed: 15795231] (f) Kim EJ, Amorelli B, Abdo M, Thomas CJ, Love DC, Knapp S, Hanover JA. *J Am Chem Soc* 2007;129:14854–5. [PubMed: 17994748] (g) Carrillo LD, Krishnamoorthy L, Mahal LK. *J Am Chem Soc* 2006;128:14768–9. [PubMed: 17105262]
3. (a) Rostovtsev VV, Green LG, Fokin VV, Sharpless KB. *Angew Chem, Int Ed* 2002;41:2596–2599. (b) Prescher JA, Bertozzi CR. *Nat Chem Biol* 2005;1:13–21. [PubMed: 16407987] (c) Speers AE, Cravatt BF. *Chem Biol* 2004;11:535–546. [PubMed: 15123248]
4. (a) Vosseller K, Trinidad JC, Chalkley RJ, Specht CG, Thalhammer A, Lynn AJ, Snedecor JO, Guan S, Medzihradzky KF, Maltby DA, Schoepfer R, Burlingame AL. *Mol Cell Proteomics* 2006;5:923–34. [PubMed: 16452088] (b) Khidekel N, Ficarro SB, Clark PM, Bryan MC, Swaney DL, Rexach JE, Sun YE, Coon JJ, Peters EC, Hsieh-Wilson LC. *Nat Chem Biol* 2007;3:339–48. [PubMed: 17496889]
5. Zachara NE, O'Donnell N, Cheung WD, Mercer JJ, Marth JD, Hart GW. *J Biol Chem* 2004;279:30133–42. [PubMed: 15138254]
6. Vocadlo DJ, Hang HC, Kim E-J, Hanover JA, Bertozzi CR. *Proc Natl Acad Sci USA* 2003;100:9116–21. [PubMed: 12874386]

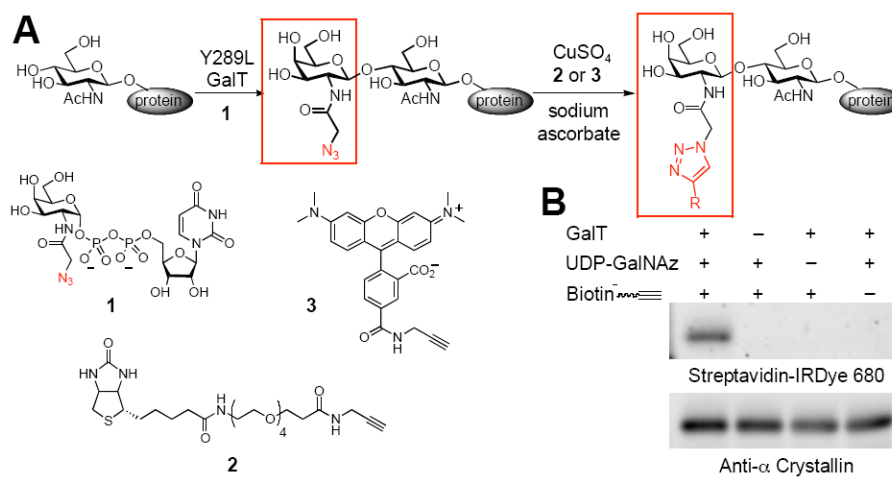


**Figure 1.**  
 (A) Chemoenzymatic labeling of *O*-GlcNAc proteins using [3+2] cycloaddition chemistry. R = biotin or TAMRA. (B) Selective labeling of  $\alpha$ -crystallin.

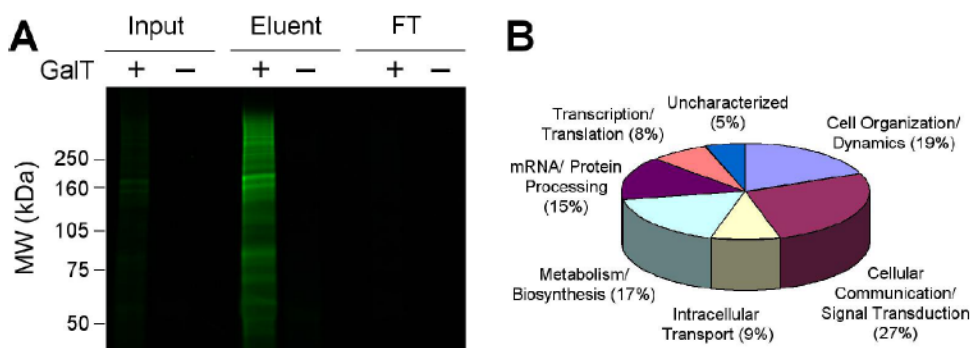


**Figure 2.**

(A) Enrichment and in-gel fluorescence detection of *O*-GlcNAc-modified proteins. 15  $\mu$ g of protein was loaded in the input and FT lanes; material captured from 470  $\mu$ g of protein was loaded in the eluent lanes. FT = flow-through. (B) Functional classification of *O*-GlcNAc proteins from rat brain identified by mass spectrometry.

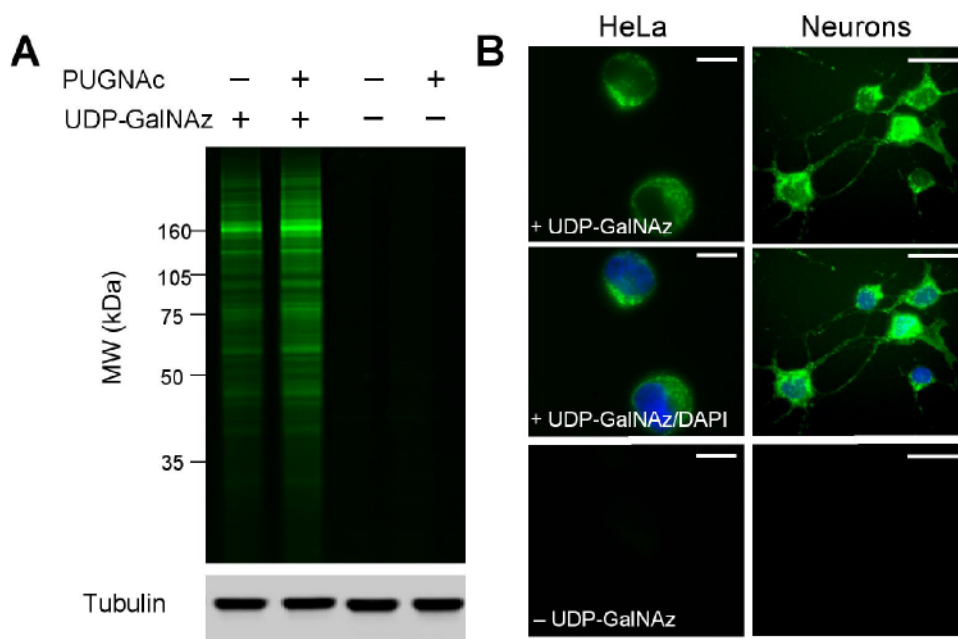


**Figure 3.** (A) Direct detection of changes in *O*-GlcNAc glycosylation levels upon cellular stimulation. Tubulin controls indicate equal loading of protein in each lane. (B) Fluorescence imaging of *O*-GlcNAc proteins (green) in HeLa cells (left) or cortical neurons (right). Nuclei were stained with DAPI (blue). Scale bars = 10  $\mu$ m (HeLa) and 25  $\mu$ m (neurons).